Supporting Information

Cu loaded NiFe layered double hydroxide bifunctional electrocatalyst with coupled interface structure for both nitrate reduction reaction and oxygen evolution reaction

Feng Du,[a] Jixin Yao,[b] Hui Luo,[a] Yanru Chen,[a] Yujie Qin,[a] Yuxin Du,[a] Yijian Wang,[a] Wei Hou,[a] Miaoxi Shuai [a] and Chunxian Guo *[a]

[a] School of Materials Science and Engineering, Suzhou University of Science and Technology, Suzhou 215009, China.
[b] Anhui Province Key Laboratory of Simulation and Design for Electronic Information System, Hefei Normal University, Hefei 230601, China.

1. Experimental

1.1 Chemicals and instruments

The chemicals are purchased from Aladdin Chemical reagent Co., Ltd. All chemicals are analytically pure grade and used as received without further purification process.

X-ray diffraction (XRD) patterns of the three catalysts were recorded at a scanning rate of 5° min^{-1} from 30° to 80° with a Cu-K radiation (λ = 0.15406 nm) using a Bruker D8 Advance powder XRD system. X-ray photoelectron spectra (XPS) measurements were performed via adopting non-monochromatized Al-Ka X-ray as the excitation source on a ThermoFisher ESCALAB Xi^+ instrument. Scanning electron microscopy (SEM) was taken to examine the morphologies of various catalysts with a Zeiss Gemini 300 instrument at 20 kV. Energy dispersive X-ray spectrometers (EDX) were detected using Oxford Ultim Max 100. Transmission electron microscopy (TEM) images and higher-resolution transmission electron microscopy (HRTEM) images were obtained with a Tecnai G2 F20 S-Twin equipped with EDAX at an acceleration voltage of 200 kV.

1.2 Electrochemical measurements

For NO_3^-RR, an electrochemical workstation (CHI660E, Chenhua, Shanghai) was adopted to perform the electrochemical tests. Typically, a H-type quartz container separated by an ion exchange membrane (nafion 117) was employed as the reaction electrolytic cell. The as-prepared electrodes, Pt foil and SCE were used as the working electrodes, counter electrode, and reference electrode, respectively.

For OER, a typical three–electrode configuration with the same CHI660E electrochemical workstation analyzer was used to evaluate OER activities in 1 M KOH electrolyte. The reference was a SCE, the counter electrode was Pt foil and the working electrodes were as–synthesized various electrocatalysts.

1.3 Detailed process for measuring ion concentration

NO_3^--N detection: First, 1.0 mL of unreacted electrolyte from the cathode cell was removed and diluted to the proper concentration for the detection range. The aforementioned solution was then gradually mixed with 1 M HCl (100 L) and 0.8 wt% sulfamic acid (10 L) before standing for 10 min. The absorbance of the produced combination was then measured using UV-Vis spectrophotometry at

220 nm and 275 nm. The calibration curve might be created by setting various KNO_3 solution concentrations and calculating the related absorbance.

NO_2^--N detection: Similar to this, post-electrolyte (1.0 mL) from the cathode cell was removed and diluted to an appropriate concentration for the detection range. After shaking thoroughly and standing for 30 minutes, color reagent (100 L) was added to the aforementioned diluent solution (5 mL). The absorbance of the combined solution was then measured using UV-Vis spectrophotometry at a wavelength of 540 nm. The calibration curve might be created by establishing various $NaNO_2$ solution concentrations and calculating the related absorbance. The following procedures were demonstrated for making color developer: Twenty grams of P-aminobenzenesulfonamide were added to a 250 mL solution of water and phosphoric acid (50 mL). The aforementioned solution was then diluted to 500 mL and transferred to a flask before receiving 1 g of N-(1-naphthyl)-ethylenediamine dihydrochloride.

NH_4^+-N detection: Postelectrolyte (1.0 mL) from the cathode cell was once more removed and diluted to an proper concentration for the detection range. After thoroughly shaking and standing for 30 minutes, 100 mL of sodium potassium tartrate solution and 150 mL of Nessler's reagent were added to the aforementioned diluent solution. In order to assess the absorbance, UV-Vis spectrophotometry at a wavelength of 420 nm was used. The calibration curve might be created by setting various NH_4Cl solution concentrations and calculating the related absorbance. The following steps were used to make sodium potassium tartrate solution (ρ = 500 $g \cdot L^{-1}$): In order to eliminate the remaining NH_4^+, sodium potassium tartrate ($KNa\text{-}C_4H_6O_6 \cdot 4H_2O$) (50 g) was dissolved in 100 mL of deionized water while being constantly stirred. The solution was finished once it had cooled to room temperature and been diluted to 100 mL.

2. Additional data

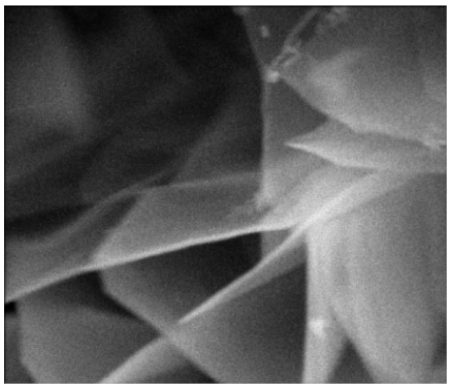

Fig. S1. SEM image for Cu/NiFe LDH.

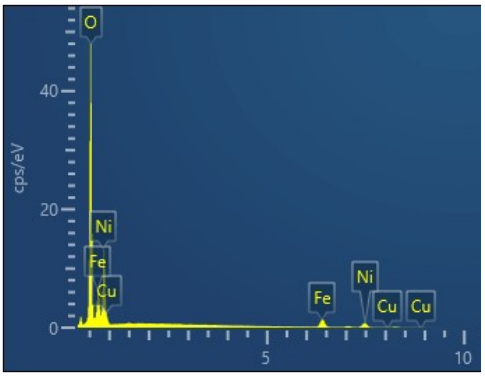

Fig. S2. EDX spectrum for Cu/NiFe LDH.

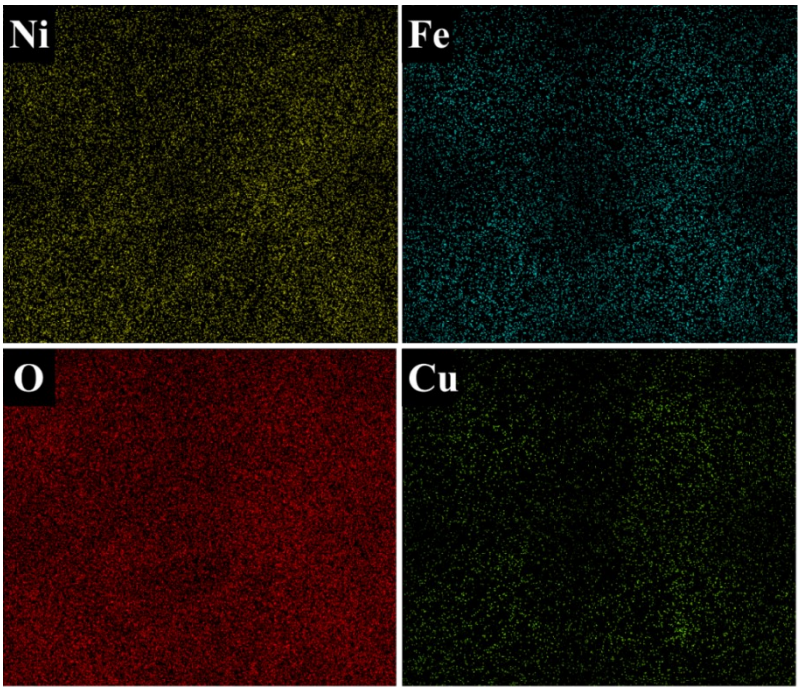

Fig. S3. EDX mappings of Ni, Fe, O and Cu for Cu/NiFe LDH.

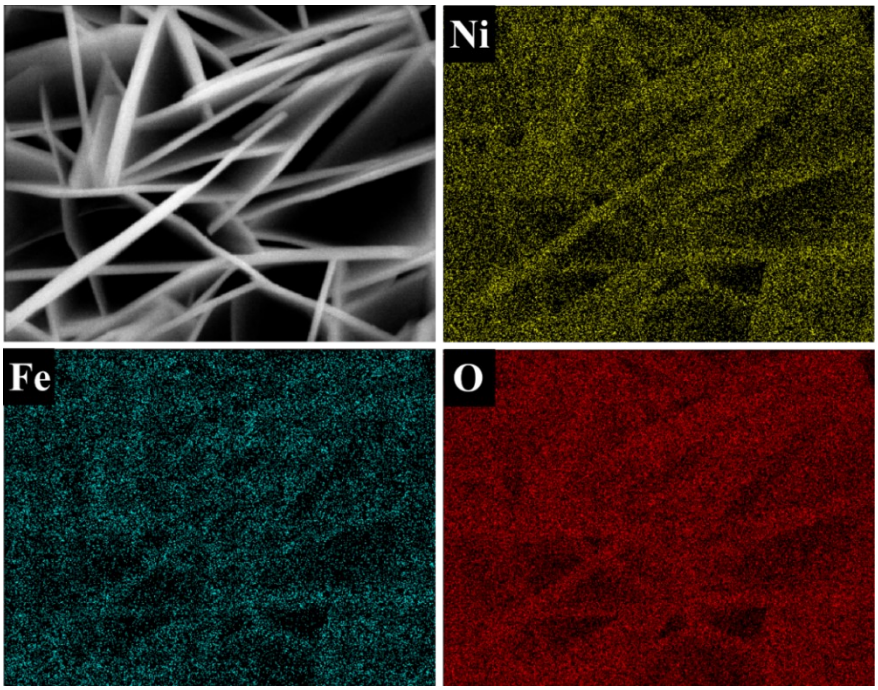

Fig. S4. SEM image and EDX mappings of Ni, Fe and O for NiFe LDH.

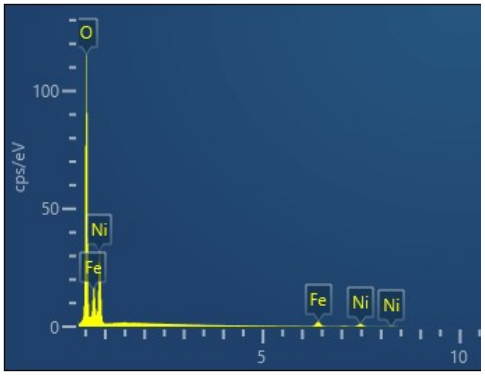

Fig. S5. EDX spectrum for NiFe LDH.

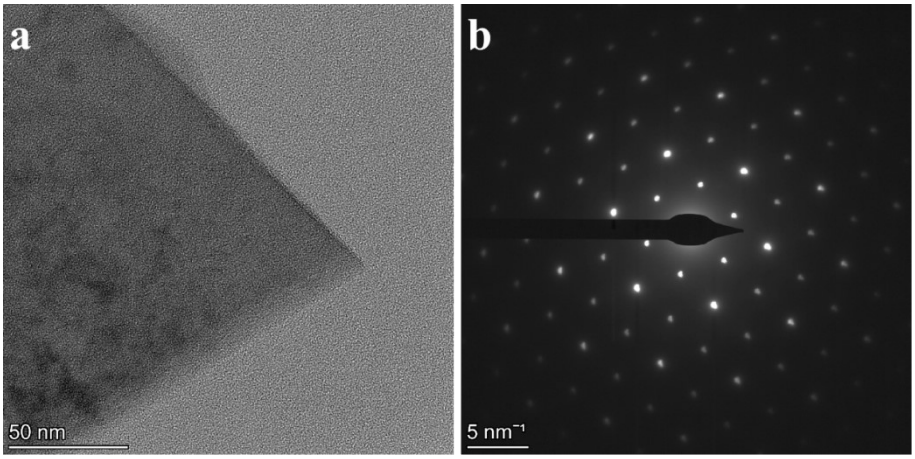

Fig. S6. (a) TEM image and (b) SAED pattern for NiFe LDH.

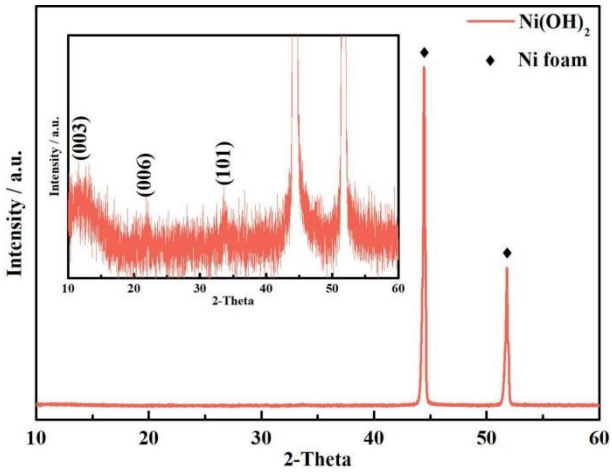

Fig. S7. XRD pattern for $Ni(OH)_2$.

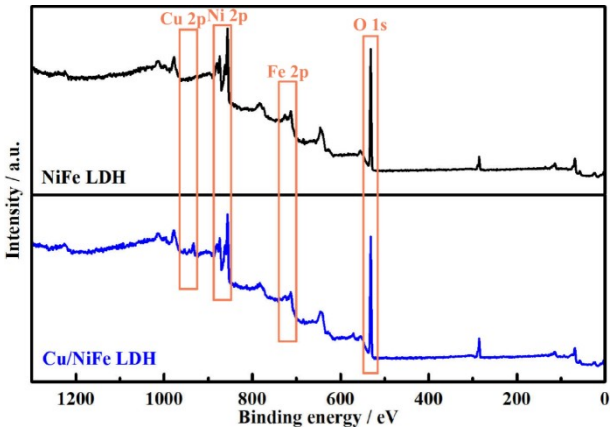

Fig. S8. XPS survey spectra for NiFe LDH and Cu/NiFe LDH.

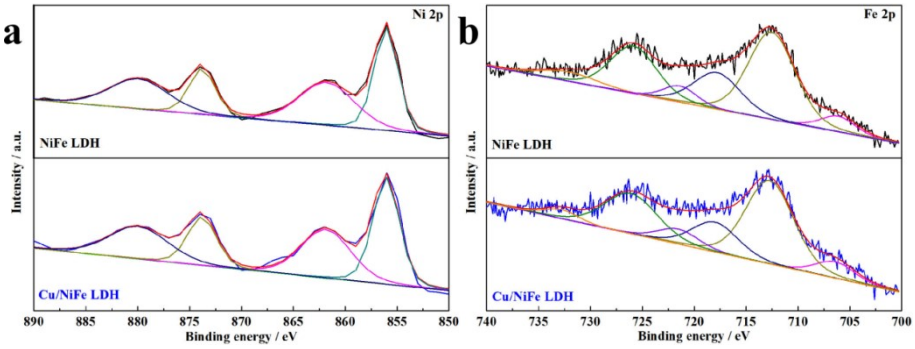

Fig. S9. XPS spectra of (a) Ni 2p and (b) Fe 2p for NiFe LDH and Cu/NiFe LDH.

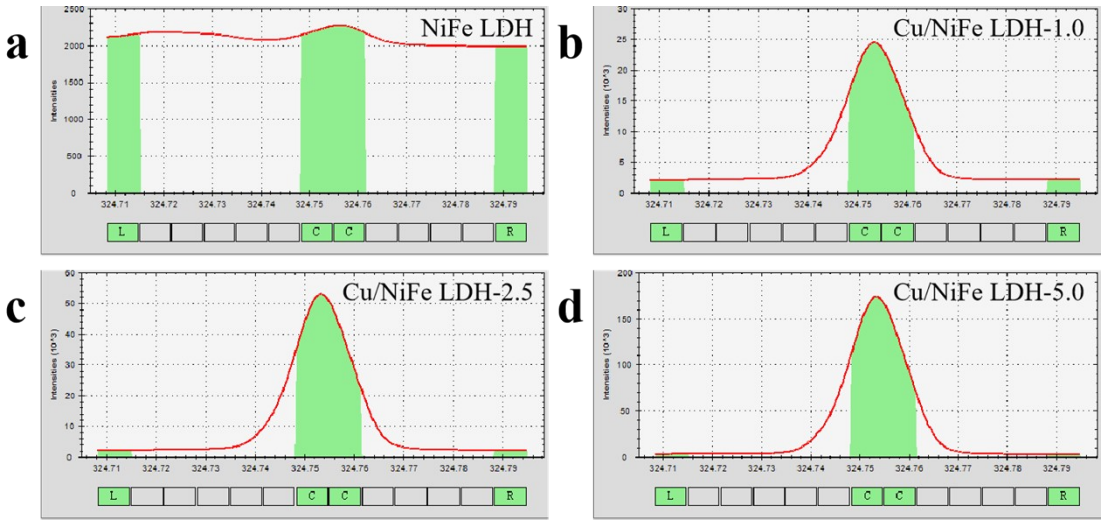

Fig. S10. The peak shapes of Cu ICP-OES lines for NiFe LDH, Cu/NiFe LDH-1.0, Cu/NiFe LDH-2.5 and Cu/NiFe LDH-5.0, respectively.

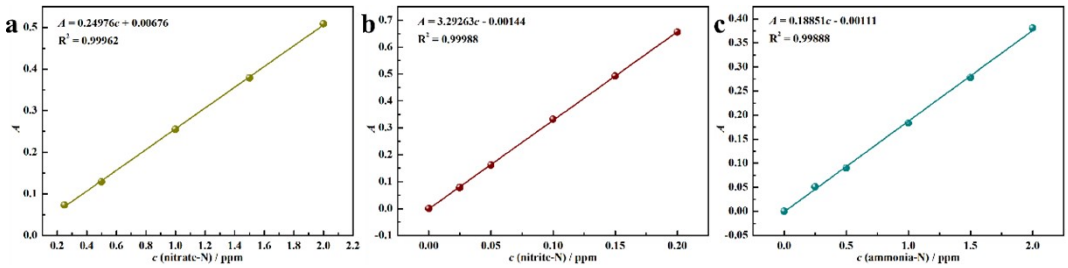

Fig. S11. The concentration-absorbance calibration curves of (a) NO_3^--N, (b) NO_2^--N and (c) NH_4^+-N. The calibration curves all show good linearity.

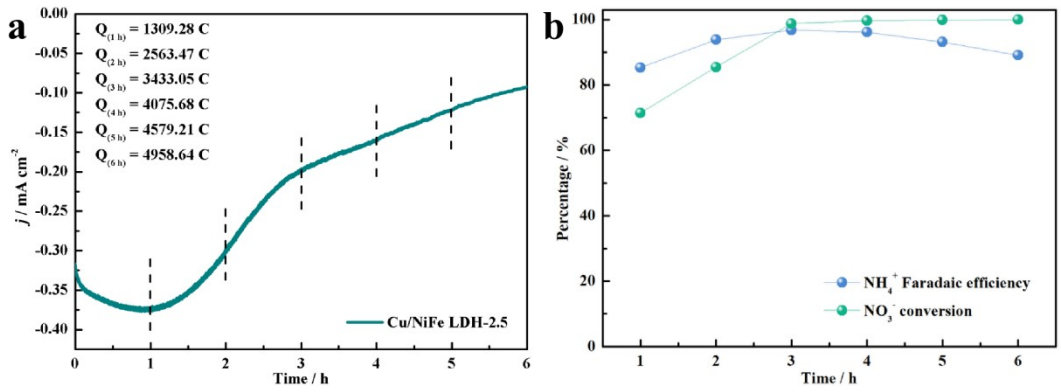

Fig. S12. (a) The 6 h chronoamperometric response measurement and (b) variation of Faraday efficiency with the 6 h chronoamperometric response measurement of Cu/NiFe LDH-2.5.

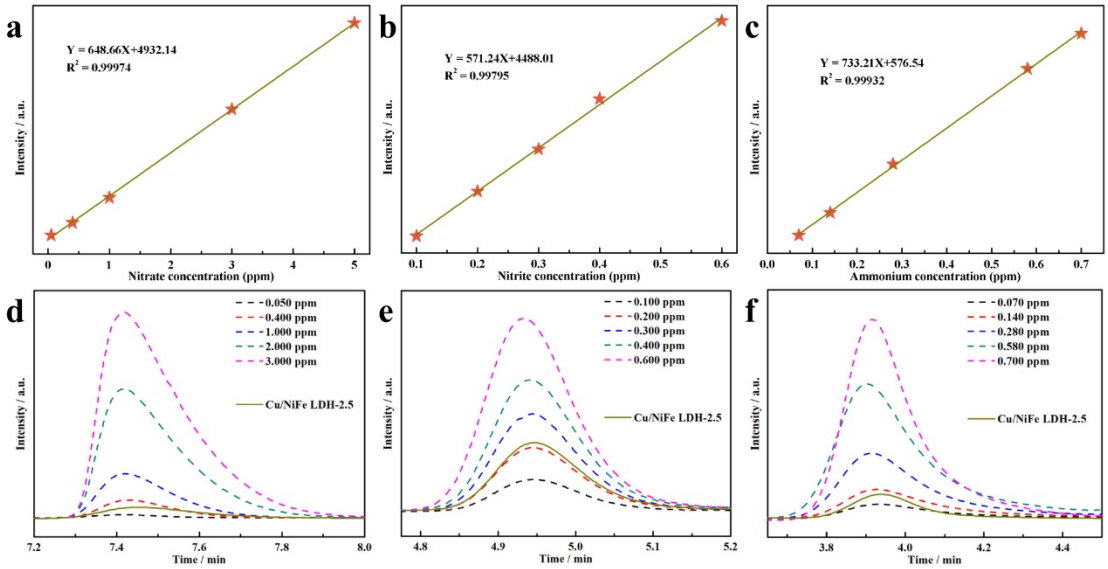

Fig. S13 (in the revised Supporting Information). (a, b and c) Calibration curve of Ion chromatogram (IC) for NO_3^-, NO_2^- and NH_3 concentrations; (d, e and f) IC curves of the time-dependent nitrate residue for a series of standard NO_3^-, NO_2^- and NH_3 solution and Cu/NiFe LDH-2.5 at -0.45 V.

Table S1. Comparison between ion chromatography and colorimetric methods for the concentration of produced nitrite and ammonium as well as residual nitrate.

	Colorimetric methods (dilution times)	**Ion chromatography (dilution times)**	**Error rate**
NO_3^--N	0.349 ppm (1000)	0.361 ppm (1000)	3.3%
NO_2^--N	0.014 ppm (1000)	0.220 ppm (60)	6.0%
NH_4^+-N	1.008 ppm (1000)	0.124 ppm (8000)	1.6%

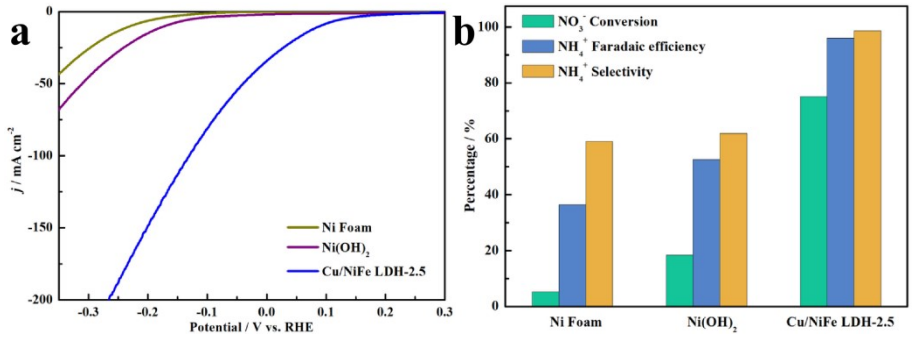

Fig. S14. (a) LSV curves and (b) activity results for Ni Foam, $Ni(OH)_2$ and Cu/NiFe LDH-2.5 with NO_3^-.

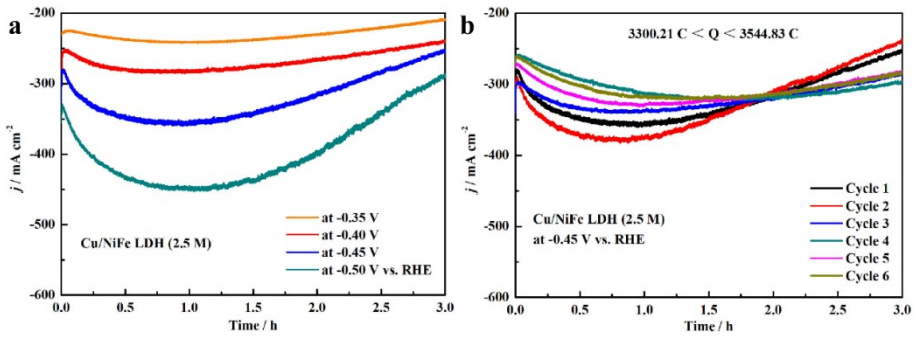

Fig. S15. (a) Four *i-t* curves at different potentials and (b) successive six *i-t* curves for Cu/NiFe LDH-2.5.

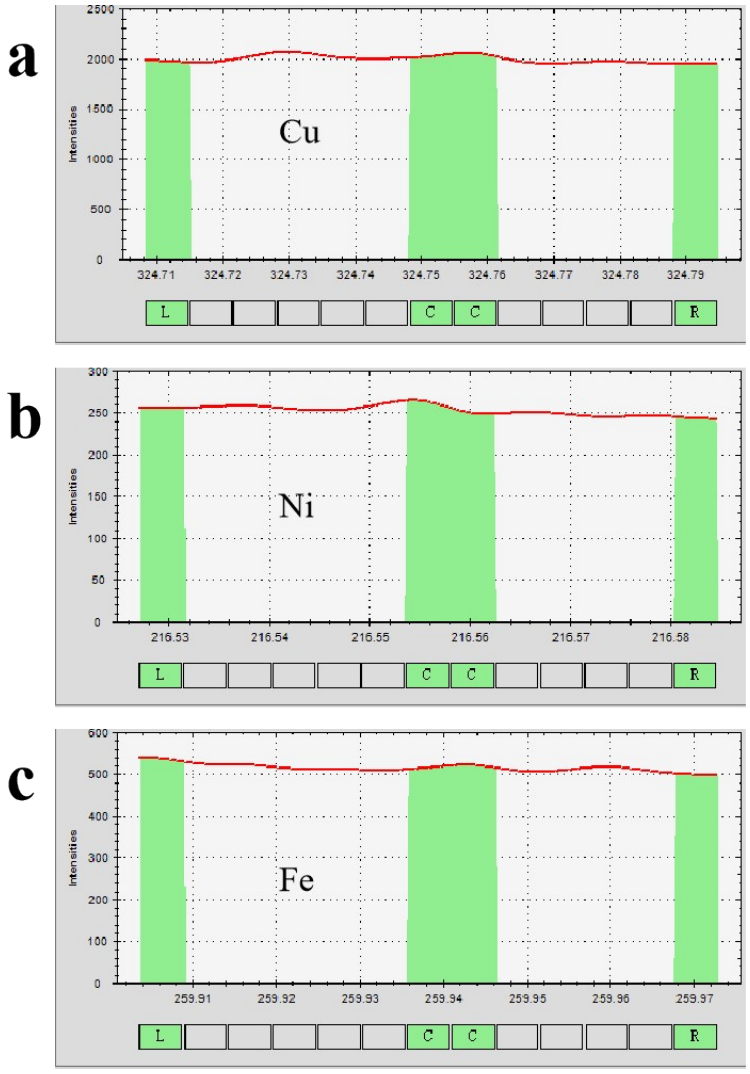

Fig. S16. The peak shapes of (a) Cu, (b) Ni and (c) Fe ICP-OES lines in the electrolyte after NO_3^-RR, respectively.

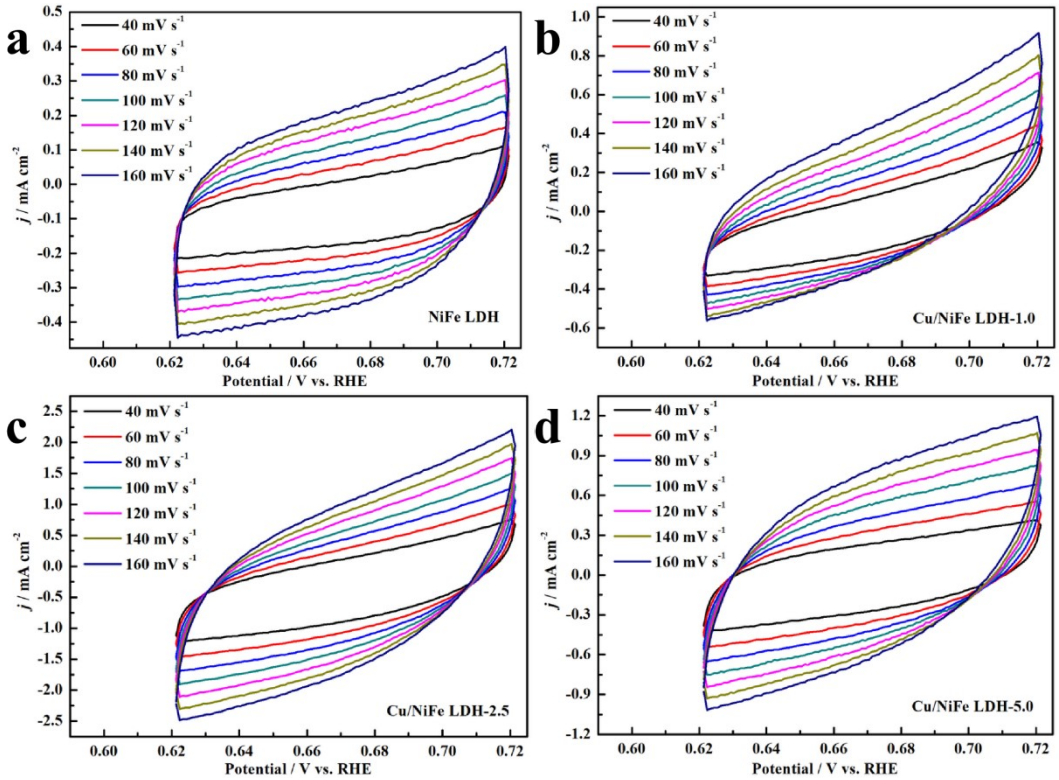

Fig. S17. CV curves for (a) NiFe LDH, (b) Cu/NiFe LDH-1.0, (c) Cu/NiFe LDH-2.5 and (d) Cu/NiFe LDH-5.0 with various scan rates from 40 to 160 mV·s^{-1}.

The measured capacitive currents were plotted as a function of scan rate in Fig. 2i and a linear fit determined the specific capacitance to be 3.16 mF·cm^{-2} for NiFe LDH, 3.59 mF·cm^{-2} for Cu/NiFe LDH-1.0, 14.22 mF·cm^{-2} for Cu/NiFe LDH-2.5 and 7.44 mF·cm^{-2} for Cu/NiFe LDH-5.0. The specific capacitance for a flat surface was generally found to be in the range of 20-60 μF·cm^{-2}. In the following calculations of electrochemical active surface area we assumed 40 μF·cm^{-2}.

$$A_{ECSA}^{\text{NiFe LDH}} = \frac{3.16\ mF \cdot cm^{-2}}{40\ \mu F \cdot cm^{-2} \cdot per\ cm_{ECSA}^{2}} = 79.00\ cm_{ECSA}^{2}$$

$$A_{ECSA}^{\text{Cu/NiFe LDH - 1.0}} = \frac{3.59\ mF \cdot cm^{-2}}{40\ \mu F \cdot cm^{-2} \cdot per\ cm_{ECSA}^{2}} = 89.75\ cm_{ECSA}^{2}$$

$$A_{ECSA}^{\text{Cu/NiFe LDH - 2.5}} = \frac{14.22\ mF \cdot cm^{-2}}{40\ \mu F \cdot cm^{-2} \cdot per\ cm_{ECSA}^{2}} = 355.50\ cm_{ECSA}^{2}$$

$$A_{ECSA}^{Cu/NiFe\ LDH\ -\ 5.0} = \frac{7.44\ mF \cdot cm^{-2}}{40\ \mu F \cdot cm^{-2} \cdot per\ cm_{ECSA}^{2}} = 186.00\ cm_{ECSA}^{2}$$

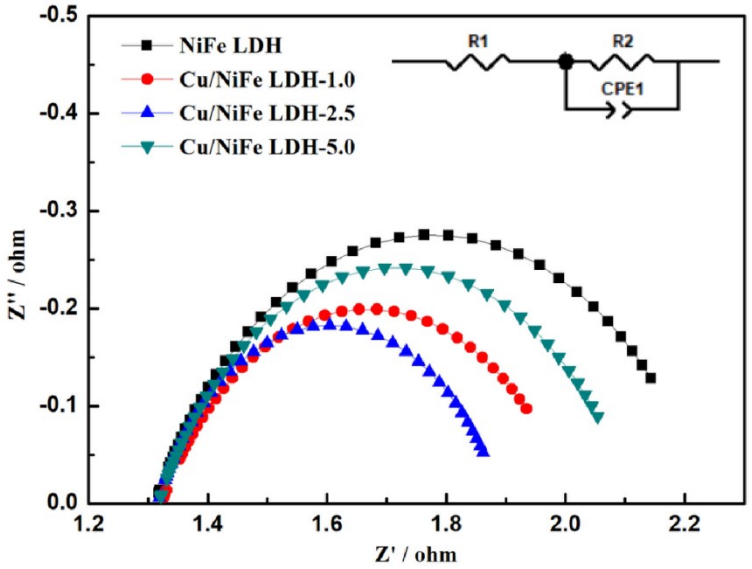

Fig. S18. The simulated curves and equivalent circuit from the Nyquist plots.

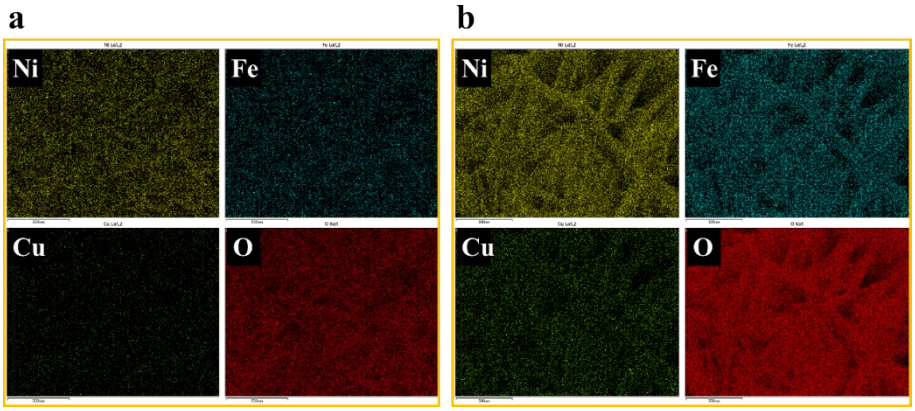

Fig. S19. EDX mappings of Ni, Fe, O and Cu for Cu/NiFe LDH after (a) NO_3^-RR and (b) OER.

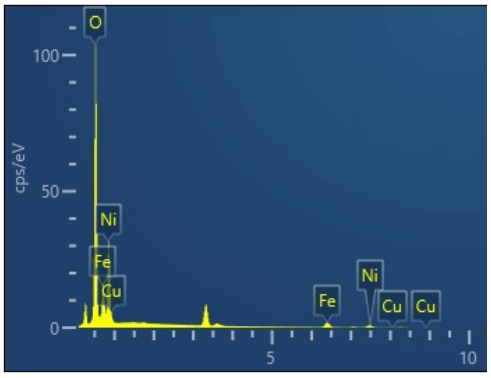

Fig. S20. EDX spectrum for Cu/NiFe LDH after NO_3^-RR.

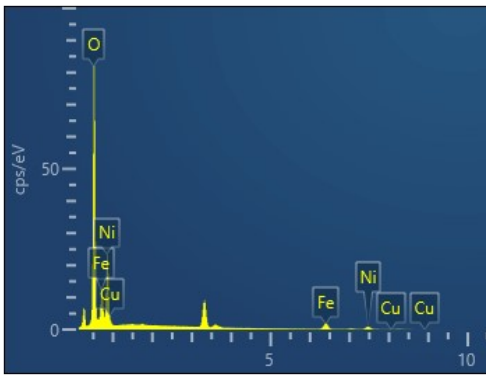

Fig. S21. EDX spectrum for Cu/NiFe LDH after OER.

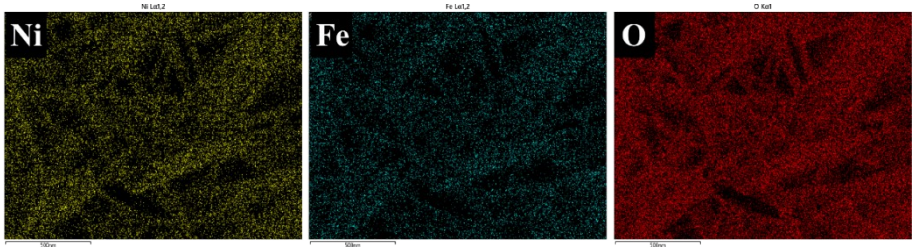

Fig. S22. EDX mappings of Ni, Fe and O for NiFe LDH after NO_3^-RR.

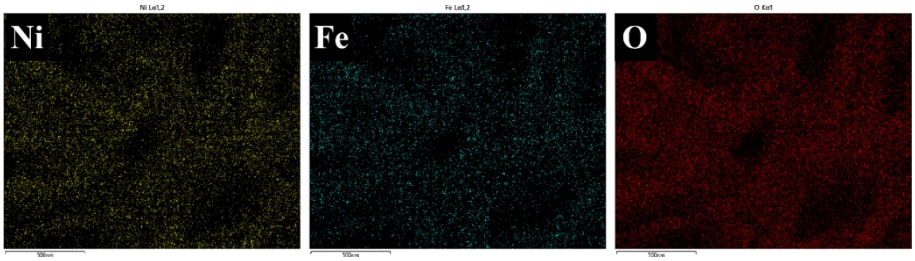

Fig. S23. EDX mappings of Ni, Fe and O for NiFe LDH after OER.

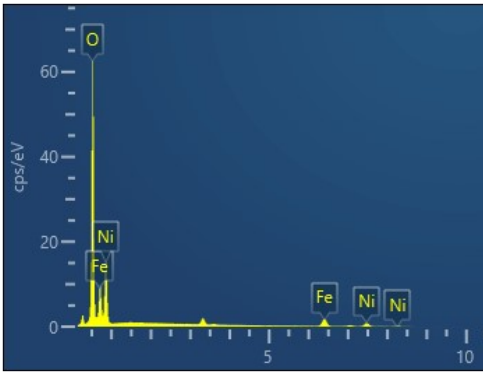

Fig. S24. EDX spectrum for NiFe LDH after NO_3^-RR.

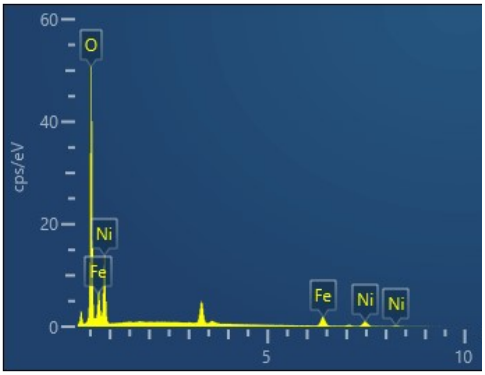

Fig. S25. EDX spectrum for NiFe LDH after OER.

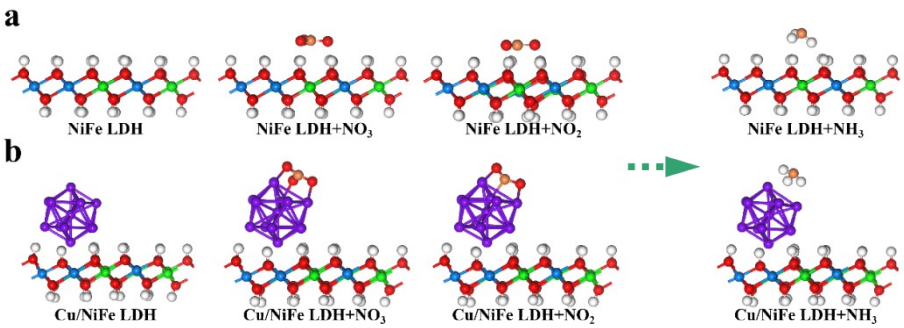

Fig. S26. Structural models of the side view for NO_3^-RR intermediates on (a) NiFe LDH and (b) Cu/NiFe LDH used in this work.